Frequency-Modulated Combs Obey a Variational Principle

Marco Piccardo,[1] Paul Chevalier,[1] Benedikt Schwarz,[1,2] Dmitry Kazakov,[1,3] Yongrui Wang,[4] Alexey Belyanin,[4] and Federico Capasso[1,*]

[1]*Harvard John A. Paulson School of Engineering and Applied Sciences, Harvard University, Cambridge, Massachusetts 02138, USA*

[2]*Institute of Solid State Electronics, TU Wien, 1040 Vienna, Austria*

[3]*Department of Information Technology and Electrical Engineering, ETH Zurich, 8092 Zurich, Switzerland*

[4]*Department of Physics and Astronomy, Texas A&M University, College Station, Texas 77843, USA*

(Received 20 November 2018; published 26 June 2019)

Laser dynamics encompasses universal phenomena that can be encountered in many areas of physics, such as bifurcation and chaos, mode competition, resonant nonlinearities, and synchronization—or locking—of oscillators. When a locking process occurs in a multimode laser, an optical frequency comb is produced, which is an optical spectrum consisting of equidistant modes with a fixed phase relationship. Describing the formation of self-starting frequency combs in terms of fundamental laser equations governing the field inside the cavity does not allow one, in general, to grasp how the laser synchronizes its modes. Our finding is that, in a particular class of lasers where the output is frequency modulated with small or negligible intensity modulation, a greatly simplified description of self-locking exists. We show that in quantum cascade lasers—solid-state representatives of these lasers characterized by an ultrashort carrier relaxation time—the frequency comb formation obeys a simple variational principle, which was postulated over 50 years ago and relies on the maximization of the laser output power. The conditions for the breakdown of this principle are also experimentally identified, shedding light on the behavior of many different types of lasers, such as dye, diode, and other cascade lasers. This discovery reveals that the formation of frequency-modulated combs is an elegant example of an optimization problem solved by a physical system.

DOI: 10.1103/PhysRevLett.122.253901

In various solid-state and gas lasers, multiple modes can reach the lasing threshold and oscillate simultaneously. These modes are in general not independent of each other but instead are coupled through a nonlinear process, such as nonlinear gain saturation of the laser medium [1] or nonlinear absorption of a saturable absorber [2], if one is present in the cavity. Mode coupling leads in turn to a well-defined phase relationship among the modes giving origin to an optical frequency comb [3–7]. These relative phases could be in principle determined by solving the coupled nonlinear equations governing the field inside the cavity, known as Lamb's self-consistency equations [8,9], but this is a nontrivial task even for the basic case of a field constituted of three modes. In the 1960s Statz, DeMars, and Tang, motivated by their observation of spiking in ruby lasers [10], investigated self-locking in multimode lasers and proposed a simplified description of this process [11,12]. This was formulated as the "maximum emission principle" (MEP) and stated that the laser operates in such way as to maximize the mean optical power output from the device [13,14]. This condition corresponds to the fastest growth of stimulated emission and thus should be established most rapidly in the laser. In terms of laser performance, it implies that the linewidth of all of the modes of the frequency comb is minimized, as this is inversely proportional to the total output power of the laser [15,16]. The MEP can be understood as follows. Consider a multimode field represented by a sinusoidally modulated waveform of period T_{rep} impinging on a slab of gain medium [Fig. 1(a)]. The dynamic response of the population inversion in the gain medium to the intensity modulation will depend, in first approximation, on how the carrier relaxation time (T_1) of the medium compares with T_{rep}. Figure 1(b) shows two limiting cases: when $T_{\mathrm{rep}} \gg T_1$, the population inversion shows large oscillations in antiphase with the intensity, and in this situation the mean extracted power is maximized for zero modulation depth; on the other hand, when T_{rep} is of the order of T_1, the phase delay between the population inversion and the intensity decreases to a value close to $\pi/2$, and the amplitude of population oscillations is suppressed. In this case the power extraction is independent of the modulation depth. In essence, the MEP can be regarded as a variational principle stating that the type of waveform chosen by the laser is the one maximizing the laser output power (see Sec. II of the Supplemental Material [17]).

Despite its intuitive appeal, the MEP is not true in general. In 1969 Schwarz and Gordon [32] employed the

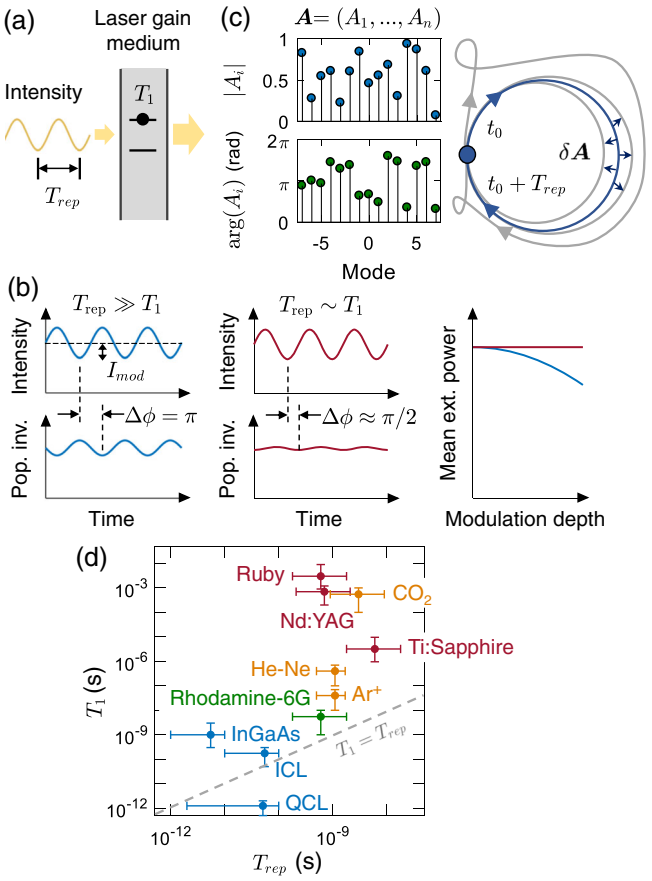

FIG. 1. Laser self-locking in terms of a variational principle. (a) An intensity modulated wave with period $T_{\rm rep}$ impinges on a slab of laser gain medium, represented as a two-level system with carrier relaxation time T_1, and becomes amplified. This modulation typically results from locking of the laser cavity modes. For simplicity, the resonator mirrors and the waveform circulation in the laser cavity are not shown. (b) Depending on how $T_{\rm rep}$ compares with T_1, the population inversion in the gain medium responds with a different amplitude and phase delay $\Delta\phi$ to the intensity modulation. The power extracted from the gain medium and averaged over $T_{\rm rep}$ is plotted as a function of the intensity modulation depth ($I_{\rm mod}$) for two limiting cases: $T_{\rm rep}\gg T_1$ (blue), $T_{\rm rep}\sim T_1$ (red). According to the maximum emission principle, the laser optimizes the phase relationship among its modes in order to maximize the extracted power. When $T_{\rm rep}\gg T_1$, this is equivalent to minimizing $I_{\rm mod}$. (c) The equations governing the field inside the laser cavity can be rewritten as the equations of motion of a dynamical system, where the generalized coordinates are the complex amplitudes of the laser (A), corresponding to (top panel) modal amplitudes and (bottom panel) phases, which are arbitrarily chosen here for illustration. Based on this formalism, the system describes a trajectory in configuration space which satisfies a variational principle for small perturbations of the motion $\delta\boldsymbol{A}$. Owing to the periodic output of frequency combs, the trajectory is a loop covered in a period $T_{\rm rep}$. (d) Characteristic timescales of the repetition period ($T_{\rm rep}$) and effective carrier relaxation time under operation (T_1) of different types of lasers: solid-state (red), semiconductor (blue), gas (orange), and dye (green) lasers.

formalism of classical mechanics to reexpress Lamb's self-consistency equations [8] as the equations of motion of a dynamical system, where the generalized coordinates correspond to the set of complex amplitudes of the laser $\boldsymbol{A}=(A_1,\ldots,A_n)$, with each giving the modulus and phase of a laser mode. Using a variational method, they restated the equations of motion of the laser as an extremum condition, which is essentially a modified form of Hamilton's principle of least action: the laser describes a trajectory in configuration space that minimizes a path integral [32] under small changes $\delta\boldsymbol{A}$ [Fig. 1(c)]. With this approach the authors showed that in general the extremum condition does not coincide with the MEP. However, they also obtained that in presence of restrictive hypotheses—in particular, if one assumes an infinitely short T_1—then the MEP and Hamilton's principle result in identical equations.

An infinitely short T_1 is a theoretical limit. This condition can be restated in terms of real laser parameters as $T_{\rm rep}\gg T_1$, where $T_{\rm rep}$ is the characteristic period of intermodal beats, usually given by the round-trip time of the laser [33] (see Sec. V of the Supplemental Material [17]). Figure 1(d) illustrates typical timescales of these parameters for common lasers [33,34]. The carrier lifetime can be shortened by the presence of light in the cavity due to stimulated emission [35,36]; here T_1 indicates the effective carrier lifetime under laser operation. Clearly, the hypothesis required for the validity of the MEP does not hold in ruby lasers due to their slow population relaxation (≈1 ms)—much longer than their round-trip time (≈1 ns)—nor does it in other solid-state lasers [e.g., neodymium-doped yttrium aluminum garnet (Nd:YAG), Ti:sapphire] or in molecular lasers (e.g., CO_2). Also appearing in Fig. 1(d) is a number of lasers which exhibit a short carrier relaxation time and lie in proximity to the $T_1=T_{\rm rep}$ line. Some of these are conventional semiconductor lasers (e.g., InGaAs-based diode lasers), while others are known as adiabatic or class-A lasers [33,37]. Examples of these lasers are He-Ne, Ar^+, rhodamine-6G, quantum cascade, and interband cascade lasers (the last have been shown to exhibit a fast dynamics only recently [38]). Some experimental studies based on different autocorrelation techniques in rhodamine-6G dye lasers [39], InAs-based Q-dash lasers [40], and interband cascade lasers [38] indicated that their output is predominantly frequency modulated [36] and that intensity modulation tends to be suppressed, in agreement with the MEP. However, in the region of the $(T_{\rm rep},T_1)$ scatter plot corresponding to these lasers, the MEP is at the limit of its applicability, and it is thus difficult to reach unambiguous conclusions on its validity.

Quantum cascade lasers (QCLs) are on the other hand an ideal model system to study the MEP, as they feature a unique combination of physical properties. In addition to an ultrashort T_1 (≈1 ps) [41], these lasers exhibit homogeneously broadened transitions and spatial hole burning effects [42], allowing multimode operation, and a resonant

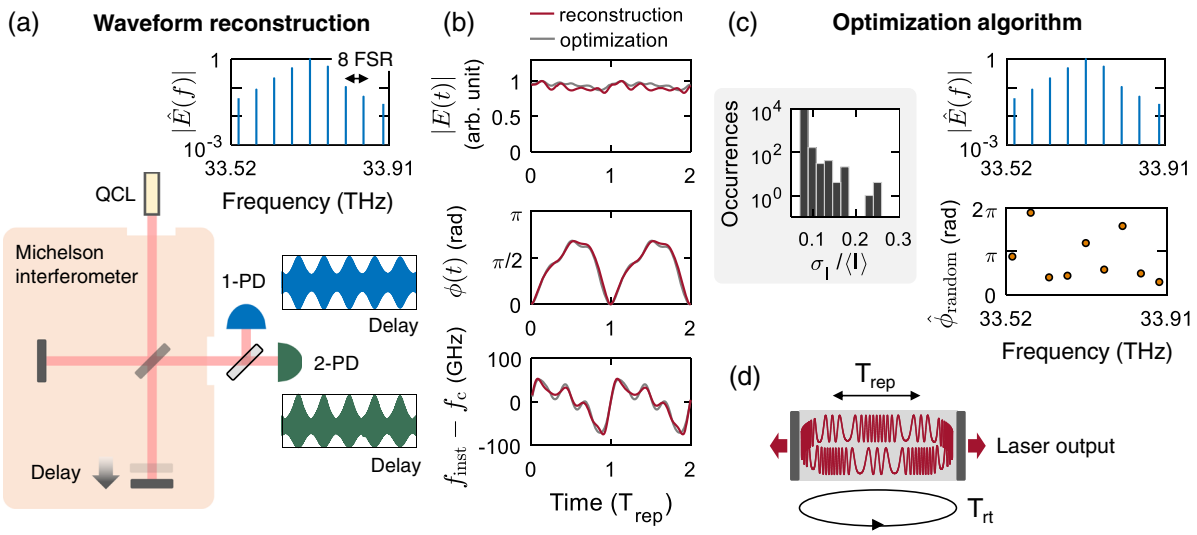

FIG. 2. Quantum cascade laser harmonic frequency comb obeying the maximum emission principle. (a) Autocorrelation measurement of a quantum cascade laser. The setup consists of a Michelson interferometer. When a linear photodetector (1-PD) measures its output as a function of interferometric delay, the linear autocorrelation trace is obtained. Its Fourier transform gives the optical spectrum of the laser, which shows a harmonic frequency comb with 8 FSR (44 GHz) skipped between the lasing modes. When the output of the interferometer is measured using a quadratic photodetector (2-PD), the second-order autocorrelation trace is obtained. Combining these measurements with a phase retrieval algorithm allows one to reconstruct the temporal waveform of the laser. (b) Amplitude, temporal phase, and instantaneous frequency (shifted by the carrier frequency of the laser, f_c) of the time-domain waveforms as obtained from the experimental reconstruction and from the best solution found by an optimization algorithm. (c) The optimization algorithm takes the spectrum of the laser and a random choice of the modal phases ($\hat{\phi}_{\mathrm{random}}$; an example is shown here) and finds the local minimum of the objective function $\sigma_I/\langle I\rangle$, where σ_I and $\langle I\rangle$ are the standard deviation and average over T_{rep} of the time-domain intensity. This is equivalent to searching the set of modal phases that minimizes intensity modulation and maximizes the laser output power. Also shown is a histogram representing the minima found over 10 000 random searches. (d) Illustration of the harmonic waveform circulating inside the laser cavity. In this example the repetition period (T_{rep}) is $1/5$ of the cavity round-trip time (T_{rt}).

third-order nonlinear susceptibility, enabling a variety of frequency comb regimes with different T_{rep} [1,43]. In this Letter we study the temporal nature of QCL frequency combs with different frequency separation between the modes by means of nonlinear autocorrelation experiments. After retrieval of the modal phases, we obtain the result that when the hypothesis $T_{\mathrm{rep}} \gg T_1$ is satisfied, the phase relationship chosen by the laser is such that it minimizes intensity modulation, thus constituting the first definite experimental verification of the MEP.

We begin by investigating QCLs operating in the harmonic frequency comb regime [44,45], where, unlike with dense frequency combs, the repetition rate $T_{\mathrm{rep}} = T_{\mathrm{rt}}/N$ is a fraction of the cavity round-trip time T_{rt} given by the number N of skipped free spectral ranges (FSRs) between the lasing modes [Fig. 2(d)]. The carrier relaxation time of these devices is $T_1 = 0.6$ ps, as calculated from band structure simulations. Our characterization of the laser waveform relies on a second-order autocorrelation measurement [46] [Fig. 2(a)]. The setup is based on a Michelson interferometer. When a linear detector is placed at its output, the optical spectrum of the QCL is obtained. Figure 2(a) shows the harmonic frequency comb generated by the first studied device, exhibiting a spacing of 8 FSR (44 GHz, $T_{\mathrm{rep}} = 23$ ps). When the output is measured by a quadratic detector, the second-order autocorrelation trace is obtained. These measurements constitute a sufficient dataset to reconstruct the temporal waveform of the laser by means of a phase retrieval algorithm [47] (see Secs. 1 and 4 of the Supplemental Material [17]). The reconstructed waveform is shown in Fig. 2(b). A nearly constant amplitude is observed, together with an approximately linear frequency chirp—a feature also seen in dense QCL frequency combs [48,49].

The temporal character of the laser output depends on the type of phase relationship existing among the modes of the frequency comb. For instance, if a linear phase relationship is arbitrarily imposed on the modes of the experimental spectrum, the laser waveform becomes a train of transform-limited pulses with a peak-to-background intensity ratio of 100 (see Fig. S5a in the Supplemental Material [17]). This raises the following question: how does the laser set its modal phases? According to the MEP, since $T_{\mathrm{rep}} \gg T_1$ for this device, it should operate in such a way as to minimize the intensity modulation [Fig. 1(b)]. We want to verify this statement. In principle one could think that both modal amplitudes and phases are degrees of freedom of the system on which the laser can act to minimize intensity modulation. If this were the case, ideal solutions would be represented by frequency-modulated (FM) and phase

modulated waves with constant amplitude, which have well-defined spectra. For instance, in the case of FM waves the spectrum is given by Bessel functions [50]. However, we argue that the laser cannot attain these ideal regimes due to constraints on the amplitudes, which originate from the specific gain profile of the laser and mechanism of multimode generation and frequency comb formation. Instead, the problem we want to solve is to find, given the experimental spectrum of the laser, the best set of modal phases which minimizes amplitude modulation. For this purpose we implement an optimization algorithm whose objective function [51] is $\sigma_I/\langle I\rangle$, where σ_I is the standard deviation of the time-domain intensity, and $\langle I\rangle$ its time-averaged value over T_{rep}. The algorithm starts with a random guess for the modal phases [Fig. 2(c)], then computes the time-domain electric field by inverse Fourier transform to evaluate the objective function and proceeds iteratively until it finds a local minimum (see Sec. I in the Supplemental Material [17]). After 10 000 random searches we find that the best solution to the optimization problem closely matches the experimentally reconstructed waveform, in terms of both the value of the objective function (7% in the optimization, 9% in the reconstruction) and the type of frequency chirp [Fig. 2(b)]. This finding indicates that the complex process of self-locking in the laser obeys the MEP.

Next, we want to investigate how the laser operates when the hypothesis $T_{\mathrm{rep}} \gg T_1$ is not satisfied. For this study we utilize a second QCL having the same T_1 of the device studied above, but operating in a harmonic frequency comb regime with a spacing of 156 GHz [28 FSR, $T_{\mathrm{rep}} = 6$ ps, Fig. 3(b)]. The phase and amplitude of population oscillations in the laser are determined by the phase and real part of the third-order nonlinear susceptibility [44], usually denoted as $\chi^{(3)}$. These quantities are calculated as a function of modulation frequency as shown in Fig. 3(a), where we marked, in particular, the $\chi^{(3)}$ response corresponding to a temporal modulation with period T_{rep} (see Sec. V in the Supplemental Material [17]). The main point to stress here is that in this frequency comb regime the population inversion can no longer follow the intensity modulation exactly in antiphase. As the MEP cannot be rigorously derived from the fundamental Hamilton's principle, it thus should start losing its validity [32]. Figure 3(c) shows the temporal waveform emitted from the QCL, which has been reconstructed using the same technique presented above. The intensity modulation depth is 16%, and the frequency chirp exhibits irregular oscillations. Interestingly, by carrying out the same optimization routine as described above, we find that a set of modal phases exists that gives a considerably smaller intensity modulation depth (3%) than the experimentally measured one [Fig. 3(c)]. This result shows that with increasing ratio of T_1/T_{rep} the MEP provides predictions that are increasingly less accurate [cf. Figs. 2(b) and 3(c)]. The laser behavior observed here, in particular the fact that amplitude

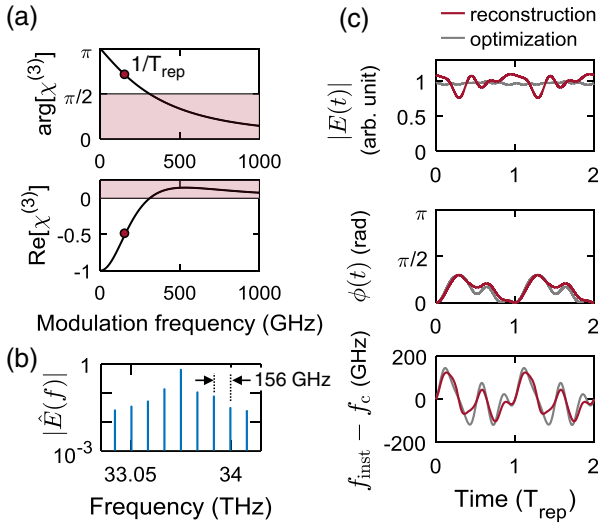

FIG. 3. The maximum emission principle starts losing its validity. (a) Phase (top panel) and real part (bottom panel) of the third-order nonlinear susceptibility $\chi^{(3)}$ as a function of modulation frequency calculated using the experimental laser parameters. The marker indicates the fundamental modulation frequency of the studied laser frequency comb having an intermodal spacing of $1/T_{\mathrm{rep}} = 156$ GHz. (b) Spectrum of the QCL operating in the harmonic regime. (c) Amplitude, temporal phase, and instantaneous frequency of the time-domain waveforms obtained from the experimental reconstruction and from the best solution found by the optimization algorithm. Unlike the case shown in Fig. 2, here the reconstruction and optimization results do not match, indicating that the maximum emission principle stops providing accurate predictions.

modulation is not perfectly minimized, is expected to be representative of other types of lasers operating in a similar region of the scatter plot of Fig. 1(d); i.e., it is close to the $T_1 = T_{\mathrm{rep}}$ line.

To further generalize our findings, we turn our attention to dense frequency combs of QCLs, in which T_{rep} is fixed by T_{rt} and is typically of the order of hundreds of picoseconds, and thus much larger than the subpicosecond T_1. We analyze the case of a self-locked midinfrared QCL frequency comb ($T_{\mathrm{rep}} = 115$ ps), whose waveform is reconstructed using a coherent beat note spectroscopy technique [48,49], giving an intensity modulation depth of 22% and a linear frequency chirp (see Sec. VI in the Supplemental Material [17]). We want to verify by means of an optimization algorithm whether the phase relationship chosen by the laser gives a minimal intensity modulation, as predicted by the MEP. This task is computationally more demanding with respect to the case of harmonic frequency combs since the much larger number of lasing modes characteristic of dense frequency combs (typically, hundreds) simultaneously increases the dimension of the configuration space and the typical iteration time of the algorithm (approximately by a factor of 1000). The best solution found over 1000 random searches lies in close

proximity to the experimental results in terms of intensity modulation depth (see Sec. VI in the Supplemental Material [17]), indicating that, to the best of our computation capabilities, the laser obeys the MEP also when operating in the dense frequency comb regime. Even though it has been known for some time that intensity tends to be suppressed at the output of QCLs [52], our studies provide a quantitative analysis of this behavior and allow one to explain it on the basis of a variational principle that can be directly deduced from the fundamental laser equations [32].

This Letter shows that a complex physical system responding to a simple variational principle can be recast as an optimization problem. This notion of the world acting as an analog computer has inspired scientists working in many different fields. For instance, such vision led Feynman to propose a universal simulator based on quantum processes [53]. In general, the goal of such optimization problems is to minimize an objective function of many variables, which may be subject to additional equality or inequality constraints. A random search of the global minimum could take an enormously long time when the number of variables is large—a concept exemplified by Levinthal's paradox in the theory of protein folding [54]—since the number of local minima typically increases exponentially with the dimension of the configuration space. It is thus fascinating that frequency-modulated combs solely responding to fundamental laws can succeed as analog optimization problem solvers.

We acknowledge support from the National Science Foundation under Grant No. ECCS-1614631. This work was performed in part at the Center for Nanoscale Systems (CNS), a member of the National Nanotechnology Coordinated Infrastructure Network (NNCI), which is supported by the National Science Foundation under NSF Grant No. 1541959. B. S. was supported by the Austrian Science Fund (FWF) within the project NanoPlas (P28914N27). We gratefully acknowledge the Lincoln Laboratory for providing QCL material. M. P. thanks A. Tassone, E. Tani, E. Moiso, and S. Cenci for discussions on optimization theory, and T. S. Mansuripur for discussions on quantum cascade lasers. Any opinions, findings, conclusions, or recommendations expressed in this material are those of the authors and do not necessarily reflect the views of the National Science Foundation.

*capasso@seas.harvard.edu

[1] J. Faist, G. Villares, G. Scalari, M. Rosch, C. Bonzon, A. Hugi, and M. Beck, Quantum cascade laser frequency combs, Nanophotonics **5**, 272 (2016).
[2] F. X. Kaertner, L. R. Brovelli, D. Kopf, M. Kamp, I. G. Calasso, and U. Keller, Control of solid state laser dynamics by semiconductor devices, Opt. Eng. **34**, 2024 (1995).
[3] T. Udem, R. Holzwarth, and T. W. Hänsch, Optical frequency metrology, Nature (London) **416**, 233 (2002).
[4] S. T. Cundiff and J. Ye, Colloquium: Femtosecond optical frequency combs, Rev. Mod. Phys. **75**, 325 (2003).
[5] T. W. Hänsch, Nobel lecture: Passion for precision, Rev. Mod. Phys. **78**, 1297 (2006).
[6] P. Del'Haye, A. Schliesser, O. Arcizet, T. Wilken, R. Holzwarth, and T. J. Kippenberg, Optical frequency comb generation from a monolithic microresonator, Nature (London) **450**, 1214 (2007).
[7] A. Hugi, G. Villares, S. Blaser, H. C. Liu, and J. Faist, Mid-infrared frequency comb based on a quantum cascade laser, Nature (London) **492**, 229 (2012).
[8] W. E. Lamb, Theory of an optical maser, Phys. Rev. **134**, A1429 (1964).
[9] M. O. Scully and M. S. Zubairy, *Quantum Optics* (Cambridge University Press, Cambridge, England, 1997).
[10] C. L. Tang, H. Statz, and G. Demars, Spectral output and spiking behavior of solid-state lasers, J. Appl. Phys. **34**, 2289 (1963).
[11] H. Statz, G. A. DeMars, D. T. Wilson, and C. L. Tang, Problem of spike elimination in lasers, J. Appl. Phys. **36**, 1510 (1965).
[12] H. Statz, G. A. DeMars, and C. L. Tang, Self-locking of modes in lasers, J. Appl. Phys. **38**, 2212 (1967).
[13] C. L. Tang and H. Statz, Maximum-emission principle and phase locking in multimode lasers, J. Appl. Phys. **38**, 2963 (1967).
[14] H. Statz, On the conditions for self-locking of modes in lasers, J. Appl. Phys. **38**, 4648 (1967).
[15] F. Cappelli, G. Campo, I. Galli, G. Giusfredi, S. Bartalini, D. Mazzotti, P. Cancio, S. Borri, B. Hinkov, J. Faist, and P. De Natale, Frequency stability characterization of a quantum cascade laser frequency comb, Laser Photonics Rev. **10**, 623 (2016).
[16] J. B. Khurgin, N. Henry, D. Burghoff, and Q. Hu, Linewidth of the laser optical frequency comb with arbitrary temporal profile, Appl. Phys. Lett. **113**, 131104 (2018).
[17] See Supplemental Material at http://link.aps.org/supplemental/10.1103/PhysRevLett.122.253901, which includes Refs. [18–31], for details on the maximum emission principle, autocorrelation measurements, the waveform reconstruction algorithm, numerical simulations of beat note power spectra, and SWIFTS measurements of dense QCL combs.
[18] A. E. Siegman, *Lasers* (University Science Books, Sausalito, CA, 1986).
[19] Y. Wang and A. Belyanin, Active mode-locking of mid-infrared quantum cascade lasers with short gain recovery time, Opt. Express **23**, 4173 (2015).
[20] M. Piccardo, D. Kazakov, N. A. Rubin, P. Chevalier, Y. Wang, F. Xie, K. Lascola, A. Belyanin, and F. Capasso, Time-dependent population inversion gratings in laser frequency combs, Optica **5**, 475 (2018).
[21] R. Trebino, K. W. DeLong, D. N. Fittinghoff, J. N. Sweetser, M. A. Krumbgel, B. A. Richman, and D. J. Kane, Measuring ultrashort laser pulses in the time-frequency domain using frequency-resolved optical gating, Rev. Sci. Instrum. **68**, 3277 (1997).
[22] C. Iaconis and I. A. Walmsley, Spectral phase interferometry for direct electric-field reconstruction of ultrashort optical pulses, Opt. Lett. **23**, 792 (1998).

[23] K. F. Lee, K. J. Kubarych, A. Bonvalet, and M. Joffre, Characterization of mid-infrared femtosecond pulses [Invited], J. Opt. Soc. Am. B **25**, A54 (2008).
[24] Q. Wu and X.-C. Zhang, Free-space electro-optics sampling of mid-infrared pulses, Appl. Phys. Lett. **71**, 1285 (1997).
[25] L. Lepetit, G. Chériaux, and M. Joffre, Linear techniques of phase measurement by femtosecond spectral interferometry for applications in spectroscopy, J. Opt. Soc. Am. B **12**, 2467 (1995).
[26] A. Bonvalet, J. Nagle, V. Berger, A. Migus, J.-L. Martin, and M. Joffre, Femtosecond Infrared Emission Resulting from Coherent Charge Oscillations in Quantum Wells, Phys. Rev. Lett. **76**, 4392 (1996).
[27] S. Bartalini, L. Consolino, F. Cappelli, G. Campo, I. Galli, D. Mazzotti, P. Cancio, G. Scalari, J. Faist, and P. De Natale, Direct measurement of the phase coherence of quantum cascade comb sources, in *Proceedings of the 2018 Conference on Lasers and Electro-Optics (CLEO), San Jose, CA, 2018* (OSA, Washington, DC, 2018).
[28] M. Piccardo, N. A. Rubin, L. Meadowcroft, P. Chevalier, H. Yuan, J. Kimchi, and F. Capasso, Mid-infrared two-photon absorption in an extended-wavelength InGaAs photodetector, Appl. Phys. Lett. **112**, 041106 (2018).
[29] H. Schneider, O. Drachenko, S. Winnerl, M. Helm, and M. Walther, Quadratic autocorrelation of free-electron laser radiation and photocurrent saturation in two-photon quantum well infrared photodetectors, Appl. Phys. Lett. **89**, 133508 (2006).
[30] D. Burghoff, T.-Y. Kao, N. Han, C. W. I. Chan, X. Cai, Y. Yang, D. J. Hayton, J.-R. Gao, J. L. Reno, and Q. Hu, Terahertz laser frequency combs, Nat. Photonics **8**, 462 (2014).
[31] J. Hillbrand, A. M. Andrews, H. Detz, G. Strasser, and B. Schwarz, Coherent injection locking of quantum cascade laser frequency combs, Nat. Photonics **13**, 101 (2019).
[32] S. E. Schwarz and P. L. Gordon, Hamilton's principle and the maximum-emission coincidence, J. Appl. Phys. **40**, 4441 (1969).
[33] Y. I. Khanin, *Principles of Laser Dynamics* (North-Holland, Amsterdam, 1995).
[34] O. Svelto, *Principles of Lasers* (Springer, New York, 2009).
[35] H. Rieck, The effective lifetime of stimulated and spontaneous emission in semiconductor laser diodes, Solid State Electron. **8**, 83 (1965).
[36] M. Dong, S. T. Cundiff, and H. G. Winful, Physics of frequency-modulated comb generation in quantum-well diode lasers, Phys. Rev. A **97**, 053822 (2018).
[37] J. R. Tredicce, F. T. Arecchi, G. L. Lippi, and G. P. Puccioni, Instabilities in lasers with an injected signal, J. Opt. Soc. Am. B **2**, 173 (1985).
[38] B. Schwarz, J. Hillbrand, M. Beiser, A. M. Andrews, G. Strasser, H. Detz, A. Schade, R. Weih, and S. Hoefling, A monolithic frequency comb platform based on interband cascade lasers and detectors, arXiv:1812.03879.
[39] L. A. Westling and M. G. Raymer, Intensity autocorrelation measurements and spontaneous FM phase locking in a multimode pulsed dye laser, J. Opt. Soc. Am. B **3**, 911 (1986).
[40] R. Rosales, S. G. Murdoch, R. Watts, K. Merghem, A. Martinez, F. Lelarge, A. Accard, L. P. Barry, and A. Ramdane, High performance mode locking characteristics of single section quantum dash lasers, Opt. Express **20**, 8649 (2012).
[41] H. Choi, L. Diehl, Z.-K. Wu, M. Giovannini, J. Faist, F. Capasso, and T. B. Norris, Gain Recovery Dynamics and Photon-Driven Transport in Quantum Cascade Lasers, Phys. Rev. Lett. **100**, 167401 (2008).
[42] A. Gordon, C. Y. Wang, L. Diehl, F. X. Kärtner, A. Belyanin, D. Bour, S. Corzine, G. Höfler, H. C. Liu, H. Schneider, T. Maier, M. Troccoli, J. Faist, and F. Capasso, Multimode regimes in quantum cascade lasers: From coherent instabilities to spatial hole burning, Phys. Rev. A **77**, 053804 (2008).
[43] M. Piccardo, P. Chevalier, T. S. Mansuripur, D. Kazakov, Y. Wang, N. A. Rubin, L. Meadowcroft, A. Belyanin, and F. Capasso, The harmonic state of quantum cascade lasers: origin, control, and prospective applications [Invited], Opt. Express **26**, 9464 (2018).
[44] T. S. Mansuripur, C. Vernet, P. Chevalier, G. Aoust, B. Schwarz, F. Xie, C. Caneau, K. Lascola, C.-E. Zah, D. P. Caffey, T. Day, L. J. Missaggia, M. K. Connors, C. A. Wang, A. Belyanin, and F. Capasso, Single-mode instability in standing-wave lasers: The quantum cascade laser as a self-pumped parametric oscillator, Phys. Rev. A **94**, 063807 (2016).
[45] D. Kazakov, M. Piccardo, P. Chevalier, T. S. Mansuripur, Y. Wang, F. Xie, C. en Zah, K. Lascola, A. Belyanin, and F. Capasso, Self-starting harmonic frequency comb generation in a quantum cascade laser, Nat. Photonics **11**, 789 (2017).
[46] T. Maier, H. Schneider, H. Liu, M. Walther, and P. Koidl, Two-photon QWIPs for quadratic detection of weak mid-infrared laser pulses, Infrared Phys. Technol. **47**, 182 (2005).
[47] K. Naganuma, K. Mogi, and H. Yamada, General method for ultrashort light pulse chirp measurement, IEEE J. Quantum Electron. **25**, 1225 (1989).
[48] M. Singleton, P. Jouy, M. Beck, and J. Faist, Evidence of linear chirp in mid-infrared quantum cascade lasers, Optica **5**, 948 (2018).
[49] D. Burghoff, Y. Yang, D. J. Hayton, J.-R. Gao, J. L. Reno, and Q. Hu, Evaluating the coherence and time-domain profile of quantum cascade laser frequency combs, Opt. Express **23**, 1190 (2015).
[50] W. M. Yee and K. A. Shore, Multimode analysis of self-locked FM operation in laser diodes, IEE Proc. J **140**, 21 (1993).
[51] I.-C. Benea-Chelmus, M. Rösch, G. Scalari, M. Beck, and J. Faist, Intensity autocorrelation measurements of frequency combs in the terahertz range, Phys. Rev. A **96**, 033821 (2017).
[52] J. B. Khurgin, Y. Dikmelik, A. Hugi, and J. Faist, Coherent frequency combs produced by self-frequency modulation in quantum cascade lasers, Appl. Phys. Lett. **104**, 081118 (2014).
[53] R. P. Feynman, Simulating physics with computers, Int. J. Theor. Phys. **21**, 467 (1982).
[54] D. J. Wales and H. A. Scheraga, Global optimization of clusters, crystals, and biomolecules, Science **285**, 1368 (1999).